



Numerical simulation of differential systems displaying rapidly oscillating solutions

I. MOISE^{1,2}, E. SIMONNET¹, R. TEMAM^{1,2} and M. ZIANE^{2,3}

¹*Laboratoire d'Analyse Numérique, Université Paris Sud, Bâtiment 425, 91405 Orsay, France*

²*The Institute for Scientific Computing and Applied Mathematics, Indiana University, Bloomington, IN 47405, USA.*

³*Center for Turbulence Research and Department of Mathematics, Stanford University, Stanford, CA 94305-3030, USA*

Received 17 August 1997; accepted in revised form 22 December 1997

Abstract. The aim of this article is to describe an approximation procedure for stiff differential equations producing highly oscillating solutions. For the sake of simplicity the presentation is restricted to ordinary differential equations. The procedure and the general approximation results are presented. Then the general results are applied to a number of simple explicit systems, for which numerical simulations of the exact and approximate solutions are performed and compared.

Keywords: stiff differential equations, oscillatory solutions, numerical simulation, systems of equations.

1. Introduction

Many phenomena in the natural sciences and engineering are described by stiff differential equations involving coefficients with different orders of magnitude which produce rapidly varying solutions. Such systems are particularly difficult (or costly) to solve numerically, since they usually demand a time step based on the smallest oscillations. Their resolution may be facilitated by the utilization of asymptotic expansions, following the methodology utilized by H. Poincaré [1] for celestial mechanics.

In this article we are interested in ordinary (finite-dimensional) differential systems that produce rapidly oscillating solutions; such systems appear for instance in the discretization of parabolic equations with superposition of waves of different lengths which are all physically significant. For example, in meteorology, the superposition of long (Rossby) waves and short (gravity) waves produces oscillations which are not easy to track and to reproduce numerically and which make predictions more difficult. Oscillations occur in many other areas of science and engineering; they occur also of course in fluid mechanics, for turbulent flows, but this is a much more complex phenomenon, which will only be briefly alluded to in this article.

This article is a preliminary report on an ongoing extended project on the analysis and numerical simulation of certain classes of differential systems displaying oscillations. To facilitate the presentation, we restrict ourselves to classes of finite-dimensional differential systems. After describing the analysis and the approximation procedure that we developed, we state the main theoretical results; we then consider some very simple model systems with two to nine variables (including a well-known five-variable model of Lorenz [2] in meteorology), and we show the results of numerical simulations based on our approximation procedure.

Underlying our work is the concept of renormalized solution of differential equations, as developed in the article by L. I. Chen, N. Goldenfeld and Y. Oono [3] and in an article of the fourth author [4] who gave a mathematical setting of the renormalization group method and proved results conjectured in [3]. Furthermore, a number of extensions and generalizations will be presented elsewhere. As is well known, many forms of renormalization have been considered elsewhere, see *e.g.* [5,6] and furthermore different aspects in [7,8,9] and in [10,11,12]. For the development of numerical methods adapted to the direct numerical simulation of rapidly oscillatory differential systems (without utilization of asymptotic expansions), see [13] and the references therein.

This article is organized as follows: in Section 2 we present the main approximation results; in Section 3 we present examples and the results of numerical simulations.

2. Description of the main results

We consider a differential system of finite dimension of the type

$$\frac{du}{dt} + Au + \frac{1}{\varepsilon}Lu + B(u, u) = f. \quad (2.1)$$

Here $u = (u_1, u_2, \dots, u_d)$ is a function from \mathbb{R}_+ into \mathbb{R}^d , $A = (A_{ij})$ is a symmetric positive-definite matrix of order d . No specific assumption is made on the matrix $L = (L_{ij})$ of order d . In the applications below L will be either a symmetric positive-definite matrix or an anti-symmetric matrix. We denote by $\rho_1, \rho_2, \dots, \rho_d$ the eigenvalues of L ; they can be complex, but we assume, for the sake of simplicity, that L can be diagonalized, which of course is the case if the eigenvalues of L are simple.

The operator B is a quadratic operator defined by its matrix (B_{jkl}) , *i.e.* using the convention of summation of repeated indices, we have

$$\{B(u, v)\}_j = B_{jkl} u_k v_l.$$

Finally, $f \in \mathbb{R}^d$ is supposed to be time-independent for the sake of simplicity, although we could handle a time-dependent term. The parameter $\varepsilon > 0$ is small compared *e.g.* to the eigenvalues of A and this is known to generate oscillations, in particular when L is antisymmetric.

We denote by $u = u^\varepsilon(t)$ the solution of the initial-value problem (2.1) consisting of (2.1) and the initial condition

$$u(0) = u_0, \quad (2.2)$$

where $u_0 \in \mathbb{R}^d$ is given.

Problems of type (2.1)–(2.2), with $L = 0$, commonly occur in the discretization of fluid-mechanics and thermohydraulics equations in the incompressible case, where B satisfies the orthogonality property

$$(B(u, v), v) = 0, \quad \forall u, v \in \mathbb{R}^d. \quad (2.3)$$

The property (2.3) of B guarantees energy conservation when A, L and f vanish and it guarantees in all cases that the solution $u = u(t)$ of (2.1)–(2.2) is defined for all positive

times. Similarly, equations of type (2.1)–(2.2) with L antisymmetric commonly appear in meteorology, where L is connected to the Coriolis force and ε is equal (or proportional) to the Rossby number which is small (see *e.g.* Pedlovsky [14]). The case where L is symmetric is also relevant and will be mentioned later on.

In view of facilitating the numerical simulation of (2.1)–(2.2) when ε is small, we are interested in approximating $u = u^\varepsilon$ for ε small; as it will appear, the solution will result from the superposition of a ‘slow’ solution based on the time scale t and a ‘fast’ solution based on the time scale $s = t/\varepsilon$ which involves the matrix $e^{(Lt/\varepsilon)}$.

We denote by P the matrix which diagonalizes L , *i.e.*

$$\tilde{L} = P^{-1}LP = \text{diag}(\rho_1, \rho_2, \dots, \rho_d).$$

As is well known, the columns of P consist of the eigenvectors φ_j of L ,

$$L\varphi_j = \rho_j\varphi_j.$$

We rewrite (2.1)–(2.2) on the basis of eigenvectors of L , *i.e.*

$$\frac{d\tilde{u}}{dt} + \tilde{A}\tilde{u} + \frac{1}{\varepsilon}\tilde{L}\tilde{u} + \tilde{B}(\tilde{u}, \tilde{u}) = \tilde{f}, \quad (2.4)$$

$$\tilde{u}(0) = \tilde{u}_0, \quad (2.5)$$

where we have set ($\tilde{u} = \tilde{u}^\varepsilon$, $u = u^\varepsilon$)

$$\begin{aligned} \tilde{u} &= P^{-1}u, & \tilde{u}_0 &= P^{-1}u_0, & \tilde{A} &= P^{-1}AP, & \tilde{f} &= P^{-1}f, \\ \tilde{B}(\cdot, \cdot) &= P^{-1}B(P\cdot, P\cdot). \end{aligned} \quad (2.6)$$

For the sake of simplicity we will first describe the approximation procedure for (2.4)–(2.5), and it will then be easy to return to (2.1)–(2.2). The first step of our renormalization procedure which will be developed in detail elsewhere, consists of defining a renormalized system for (2.1) which reads in the present case

$$\frac{d\tilde{U}}{dt} + \tilde{A}_0\tilde{U} + \tilde{B}_0(\tilde{U}, \tilde{U}) = \tilde{f}_0, \quad (2.7)$$

$$\tilde{U}(0) = \tilde{u}_0. \quad (2.8)$$

Note that related systems appear elsewhere under the name of averaged systems, see *e.g.* V.I. Arnold [15,16], A Bensoussan, J.L. Lions and G. Papanicolaou [17], and the references mentioned in the introduction.

In (2.7), the matrix \tilde{A}_0 is defined by its elements

$$\tilde{A}_{0jk} = \begin{cases} \tilde{A}_{jk} & \text{if } \rho_j = \rho_k, \\ 0 & \text{otherwise;} \end{cases}$$

in particular \tilde{A}_0 is diagonal if all ρ_i are distinct. Similarly, \tilde{f}_0 is defined by its components

$$\tilde{f}_{0j} = \begin{cases} \tilde{f}_j & \text{if } \rho_j = 0, \\ 0 & \text{otherwise;} \end{cases}$$

finally

$$\{\tilde{B}_0(\tilde{U}, \tilde{V})\}_j = \tilde{B}_{0jkl} \tilde{U}_k \tilde{V}_l,$$

with

$$\tilde{B}_{0jkl} = \begin{cases} \tilde{B}_{jkl} & \text{if } \rho_j = \rho_k + \rho_l, \\ 0 & \text{otherwise.} \end{cases}$$

The analogue of (2.3) does not hold necessarily for (2.7)–(2.8) and the existence of $U(t)$ for all time $t > 0$ is not straightforward; we will assume the existence of $U(t)$ which is easy to verify in the examples below.

We now define the approximate solution $\tilde{u}^\varepsilon(t)$; it reads:

$$\tilde{u}^\varepsilon(t) = e^{-\tilde{L}t/\varepsilon} \left\{ \tilde{U}(t) + \varepsilon \tilde{F}_3\left(\frac{t}{\varepsilon}, \tilde{U}(t)\right) \right\} \quad (2.9)$$

The definition of F_3 is as follows: we write

$$\tilde{F}(v) = \tilde{f} - \tilde{B}(\tilde{v}, \tilde{v}) - \tilde{A}v,$$

and

$$\begin{aligned} e^{\tilde{L}s} \tilde{F}(e^{-\tilde{L}s}v) &= \tilde{F}_1(v) + \tilde{F}_2(s, v), \\ \int_0^s e^{\tilde{L}\sigma} \tilde{F}(e^{-\tilde{L}\sigma}v) d\sigma &= \tilde{F}_1(v)s + \tilde{F}_3(s, v), \end{aligned} \quad (2.10)$$

i.e. bearing in mind the form of \tilde{F} and of $e^{\tilde{L}\sigma}$, $\tilde{F}_3(s, v)$ is the part of the left-hand side of (2.10) which is not a linear function of s ; this is the nonresonant part in the left-hand side of (2.10); the resonant part appears in \tilde{F}_1 ,

$$\tilde{F}_1(v) = \tilde{f}_0 - \tilde{A}_0v - \tilde{B}_0(v, v). \quad (2.11)$$

Note that

$$\tilde{u}^\varepsilon(0) = \tilde{u}_0 \quad (2.12)$$

since $\tilde{F}_3(0, v) = 0$ (by (2.10)) and $\tilde{U}(0) = \tilde{u}(0)$.

Inserting now \tilde{u}^ε into Equation (2.4), we can write

$$\frac{d\tilde{u}^\varepsilon}{dt} + \tilde{A}\tilde{u}^\varepsilon + \frac{1}{\varepsilon}\tilde{L}\tilde{u}^\varepsilon + \tilde{B}(\tilde{u}^\varepsilon, \tilde{u}^\varepsilon) = \tilde{f} + \varepsilon\tilde{R}_\varepsilon, \quad (2.13)$$

and we have

THEOREM 1. *On every interval $[0, T]$, the function $\tilde{R}_\varepsilon = \tilde{R}_\varepsilon(t)$ is bounded, independently of t and ε .*

Then, for the error $\tilde{u}^\varepsilon - \tilde{u}$:

THEOREM 2. *There exists a constant \tilde{K}_T depending on T and on the data, but independent of ε , such that*

$$\sup_{t \in [0, T]} |\tilde{u}^\varepsilon(t) - \tilde{u}^\varepsilon(t)| \leq \varepsilon \tilde{K}_T.$$

The proofs of these theorems will appear elsewhere [18]. \square

Let us now reinterpret this result in terms of the initial vector function $u = u^\varepsilon$ and of the initial system (2.1)–(2.2); this only necessitates rewriting the renormalized system (2.7) and reinterpreting formula (2.9) in the initial basis.

First, setting $U = U(t) = P\tilde{U}(t)$, we infer from (2.7)–(2.8) that U solves to the following system

$$\frac{dU}{dt} + A_0 U + B_0(U, U) = f_0, \quad (2.14)$$

$$U(0) = u_0, \quad (2.15)$$

where A_0, B_0, f_0 are defined as follows:

$$A_0 = P\tilde{A}_0P^{-1}, \quad f_0 = P\tilde{f}_0, \quad B_0(\cdot, \cdot) = PB_0(P^{-1}\cdot, P^{-1}\cdot), \quad (2.16)$$

i.e. componentwise:

$$A_{0ij} = \sum_{\substack{\alpha, \beta, \gamma, \delta \\ \rho_\alpha = \rho_\beta}} P_{i\alpha} P_{\alpha\gamma}^{-1} A_{\gamma\delta} P_{\delta\beta} P_{\beta j}^{-1}, \quad f_{0i} = \sum_{\substack{\alpha, \beta \\ \rho_\alpha = 0}} P_{i\alpha} P_{\alpha\beta}^{-1} f_\beta,$$

$$\{B_0(U, V)\}_i = B_{0ijk} U_j V_k, \quad B_{0ijk} = \sum_{\substack{\alpha, \beta, \gamma, \delta, \lambda, \mu \\ \rho_\alpha = \rho_\beta + \rho_\gamma}} P_{i\alpha} P_{\alpha\delta}^{-1} B_{\delta\lambda\mu} P_{\lambda\beta} P_{\beta j}^{-1} P_{\mu\gamma} P_{\gamma k}^{-1},$$

Then we define the approximation $\tilde{u}^\varepsilon = P\tilde{u}^\varepsilon$: the initial system (2.1) is written in the equivalent form

$$\frac{du}{dt} + \frac{1}{\varepsilon} Lu = F(u), \quad (2.17)$$

where

$$F(u) = f - Au - B(u, u);$$

we then set

$$F(v) = F_1(v) + F_2(s, v), \quad \int_0^s e^{L\sigma} F(e^{-L\sigma} v) d\sigma = F_1(v)s + F_3(s, v); \quad (2.18)$$

namely $F_3(s, v)$ consists of the part of the left-hand side of (2.18) which is not a linear function of s . Of course, this definition makes sense only if we bear in mind the form of $e^{L\sigma}$ and the quadratic form of F .

Now we set

$$\bar{u}^\varepsilon(t) = P\bar{\tilde{u}}^\varepsilon = e^{-Lt/\varepsilon} \left\{ U(t) + \varepsilon F_3 \left(\frac{t}{\varepsilon}, U(t) \right) \right\} \quad (2.19)$$

Clearly (2.13) and (2.19) show that

$$\frac{d\bar{u}^\varepsilon}{dt} + A\bar{u}^\varepsilon + \frac{1}{\varepsilon}L\bar{u}^\varepsilon + B(\bar{u}^\varepsilon, \bar{u}^\varepsilon) = f + \varepsilon R_\varepsilon, \quad (2.20)$$

$$\bar{u}^\varepsilon(0) = u_0, \quad (2.21)$$

with

$$R_\varepsilon = P\tilde{R}_\varepsilon.$$

Then, Theorems 1 and 2 are easily reinterpreted in the following form:

THEOREM 1'. *On every interval $[0, T]$, the function $R_\varepsilon = R_\varepsilon(t)$ is bounded, independently of t and ε .*

THEOREM 2'. *There exists a constant K_T depending on T and on the data, but independent of ε , such that*

$$\sup_{t \in [0, T]} |u^\varepsilon(t) - \bar{u}^\varepsilon(t)| \leq \varepsilon K_T.$$

Remark 1. We recall that, for Theorems 1, 2, 1', 2', we have assumed that $U(t)$ (or $\tilde{U}(t)$) is defined for all $t \in [0, T]$ (or, more generally, for all $t \geq 0$). This assumption needs to be justified for each specific example.

3. Applications

We now apply Theorems 1' and 2' to a few finite-dimensional systems. In general, in the numerical examples, our aim is to show how effective the approximation of u^ε by \bar{u}^ε is and, thus, we will compare some (oscillatory) components of u^ε and \bar{u}^ε . However, as far as the practical interest of the method is concerned, we have to keep in mind that $\bar{u}^\varepsilon(t)$ is computed by (2.19). The main term is $U(t)$ which is a solution of the nonoscillatory Equation (2.14), that we then multiply by the oscillatory matrix $e^{-Lt/\varepsilon}$. In a few cases we have plotted an oscillatory component of u^ε and compared it to the corresponding (non-oscillatory) component of U . Numerical integration of the very simple system (2.14) is made by an implicit Crank–Nicolson scheme.

EXAMPLE 1. In this example $d = 3$ and, setting $u = (x, y, z)$, we have that the initial system (2.1) reads

$$\begin{cases} \dot{x} + \lambda_1 x + \frac{1}{\varepsilon}(y + z) + x(y + z) - y^2 - z^2 = f, \\ \dot{y} + \lambda_2 y - \frac{1}{\varepsilon}x + xy - x^2 = g, \\ \dot{z} + \lambda_3 z - \frac{1}{\varepsilon}x + xz - x^2 = h. \end{cases} \quad (3.1)$$

After straightforward calculations, we obtain the analogue of Equation (2.7) (in the initial basis), namely

$$\begin{cases} \dot{X} + \frac{1}{4}(2\lambda_1 + \lambda_2 + \lambda_3)X = 0, \\ \dot{Y} + \frac{1}{8}(2\lambda_1 + 3\lambda_2 + 3\lambda_3)Y + \frac{1}{8}(2\lambda_1 - \lambda_2 - \lambda_3)Z = \frac{1}{2}(g - h), \\ \dot{Z} + \frac{1}{8}(2\lambda_1 - \lambda_2 - \lambda_3)Y + \frac{1}{8}(2\lambda_1 + 3\lambda_2 + 3\lambda_3)Z = -\frac{1}{2}(g - h). \end{cases} \quad (3.2)$$

Remark 2. Note that (3.2) is a linear system. \square

In the numerical simulations shown below, we have chosen $\lambda_1 = 10^{-2}$, $\lambda_2 = 10^{-1}$, $\lambda_3 = 1$, $f = 0.5$, $g = 0.9$, $h = 0.7$ and $\varepsilon = 5 \times 10^{-3}$.

We show hereafter in Figure 1 the results of numerical simulations comparing some components of the exact solution $u^\varepsilon = u = (x, y, z)$ and of its approximation $\bar{u}^\varepsilon = \bar{u} = (\bar{x}, \bar{y}, \bar{z})$. More precisely, Figure 1(a) shows the slow mode $y - z$ and the fast mode $y + z$ and their approximations $\bar{y} - \bar{z}$ and $\bar{y} + \bar{z}$. Figure 1(b) shows a zoom of a section of Figure 1(a) corresponding to $y + z$ and $\bar{y} + \bar{z}$, on which the difference between the two curves can be seen.

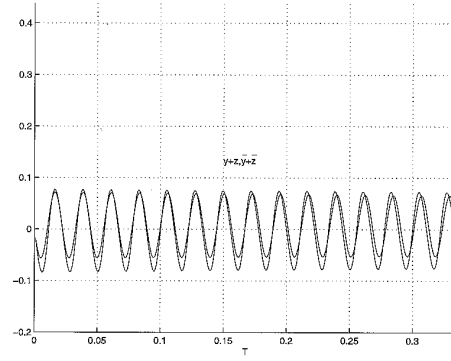
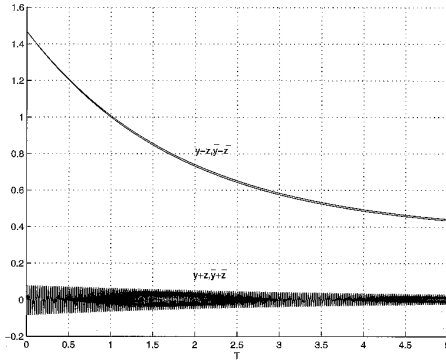


Figure 1(a). Comparison of the exact and approximate solutions.

Figure 1(b). Zoom of a section of (a).

EXAMPLE 2. The following system is a slightly different version of Example 1:

$$\begin{cases} \dot{x} + \lambda_1 x - \frac{1}{\varepsilon}y - (ax + by)z = f, \\ \dot{y} + \lambda_2 y + \frac{1}{\varepsilon}x + (bx - dy)z = g, \\ \dot{z} + \lambda_3 z + ax^2 + dy^2 = h. \end{cases} \quad (3.3)$$

For this example, the renormalized system reads:

$$\begin{cases} \dot{X} + \frac{1}{2}(\lambda_1 + \lambda_2)X - \frac{1}{2}(a + d)XZ - bYZ = 0, \\ \dot{Y} + \frac{1}{2}(\lambda_1 + \lambda_2)Y - \frac{1}{2}(a + d)YZ + bXZ = 0, \\ \dot{Z} + \lambda_3 Z + \frac{1}{2}(a + d)(X^2 + Y^2) = h. \end{cases} \quad (3.4)$$

Note that, in this case, the renormalized system is, in general, nonlinear (*i.e.*, if $a + d \neq 0$ or $b \neq 0$). \square

We show hereafter in Figure 2 the results of numerical simulations comparing some components of the exact solution $u^\varepsilon = u = (x, y, z)$ and of its approximation $\bar{u}^\varepsilon = \bar{u} = (\bar{x}, \bar{y}, \bar{z})$; in Figure 2(a) the slow mode z, \bar{z} appears in bold line, the fast mode x, \bar{x} corresponds to the lighter (highly oscillating) line. Figure 2(b) shows the zoom of a section of Figure 2(a), in which the difference between z and \bar{z} appears clearly. Note also the small oscillations of z which have been averaged in \bar{z} . Figure 2(c) shows the superposition of x, X and Y , where X and Y are two nonoscillatory components of the renormalized solution $U = (X, Y, Z)$. Here, the approximations \bar{x} and \bar{y} of x, y satisfy the relations: $\bar{x} = \cos(t/\varepsilon)X + \sin(t/\varepsilon)Y$ and $\bar{y} = -\sin(t/\varepsilon)X + \cos(t/\varepsilon)Y$. We did not plot here y, \bar{y} and \bar{x} , because of the slight phase differences which would make the figure too dark.

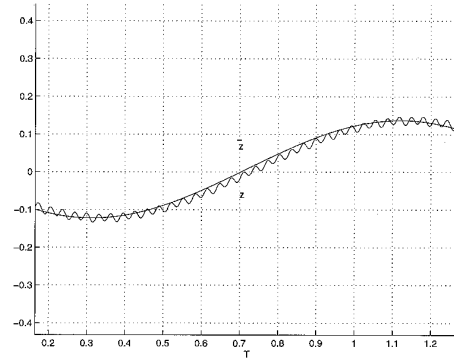
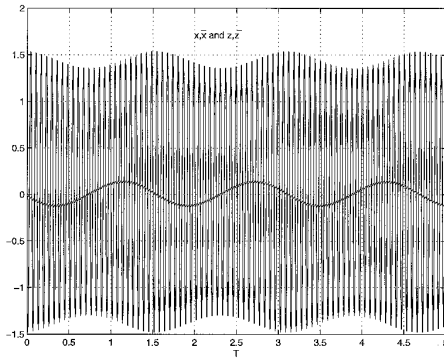


Figure 2(a). Comparison of the exact and approximate solutions.

Figure 2(b). Zoom of a section of (a).

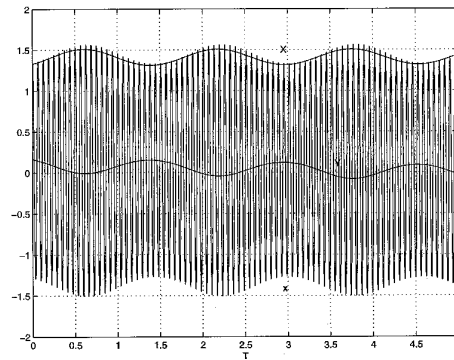


Figure 2(c). Comparison of x, X and Y .

For the numerical simulations shown below, we have chosen $\lambda_1 = 10^{-2}$, $\lambda_2 = 2 \times 10^{-2}$, $\lambda_3 = 10^{-2}$, $f = 2$, $g = 3$, $h = 4$, $a = 1$, $b = 2$, $d = 3$ and $\varepsilon = 10^{-2}$.

EXAMPLE 3. This is a five-equations system proposed by E. Lorenz [2] for meteorology. We change notations and set $u = (U, V, W, X, Z)$ and replace U by $(U^*, V^*, W^*, X^*, Z^*)$. The initial system reads:

$$\begin{cases} \dot{U} + \lambda_1 U + VW - bVZ = 0, \\ \dot{V} + \lambda_1 V - 2UW + 2bUZ = F, \\ \dot{W} + \lambda_1 W + UV = 0, \\ \dot{X} + \lambda_2 X + \frac{1}{\varepsilon} Z = 0, \\ \dot{Z} + \lambda_2 Z - \frac{1}{\varepsilon} X - bUV = 0. \end{cases} \quad (3.5)$$

Our analysis leads to the following renormalized system:

$$\begin{cases} \dot{U}^* + \lambda_1 U^* + V^* W^* = 0, \\ \dot{V}^* + \lambda_1 V^* - 2U^* W^* = F, \\ \dot{W}^* + \lambda_1 W^* + U^* V^* = 0, \\ \dot{X}^* + \lambda_2 X^* = 0, \\ \dot{Z}^* + \lambda_2 Z^* = 0. \end{cases} \quad (3.6)$$

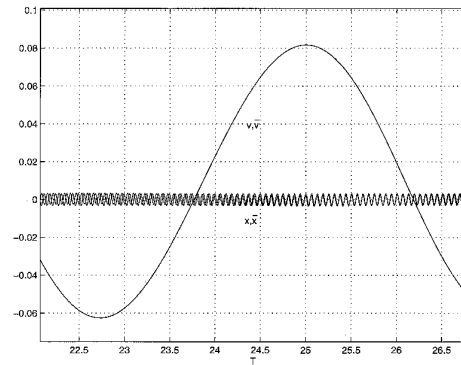
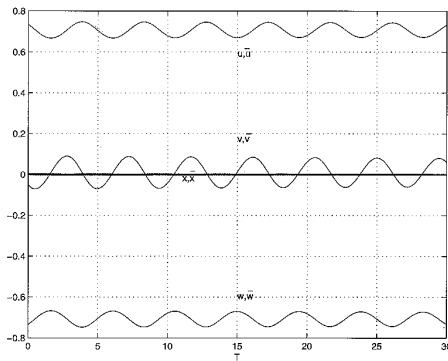


Figure 3(a). Comparison of the exact and approximate solutions.

Figure 3(b). Zoom of a section of (a).

In the numerical simulations shown below we have chosen $\lambda_1 = \lambda_2 = 10^{-2}$, $b = 1$, $F = 1$, $\varepsilon = 10^{-2}$. Figure 3(a) shows U, V, W, X and their approximations $\bar{U}, \bar{V}, \bar{W}, \bar{X}$. Figure

3(b) shows a zoom of part of Figure 3(a) for X, \bar{X} and V, \bar{V} . The differences between V and \bar{V} are not noticeable; those between X and \bar{X} are apparent.

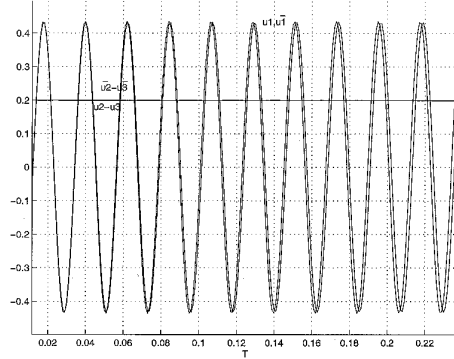


Figure 4(a). Comparison of the exact and approximate solutions.

EXAMPLE 4. We consider now a nine-equation model. We set $u = (u_1, \dots, u_9)$, and write for $i = 1, 4, 7$ ($u_{\alpha+9} = u_\alpha, \alpha = 1, \dots, 9$):

$$\begin{aligned} \dot{u}_i + (u_{i+3}^2 - u_i u_{i+6}) + \nu u_i + \frac{1}{\varepsilon}(u_{i+1} + u_{i+2}) &= F, \\ \dot{u}_{i+1} + (u_{i+2}^2 - u_{i+1} u_{i+2}) + c \nu u_{i+1} - \frac{1}{\varepsilon} u_i &= 0, \\ \dot{u}_{i+2} + (u_{i+1}^2 - u_{i+1} u_{i+2}) + c \nu u_{i+2} - \frac{1}{\varepsilon} u_i &= 0. \end{aligned} \tag{3.7}$$

For this example we have

$$L = \begin{pmatrix} L_I & 0 & 0 \\ 0 & L_I & 0 \\ 0 & 0 & L_I \end{pmatrix}, \quad P = \begin{pmatrix} P_I & 0 & 0 \\ 0 & P_I & 0 \\ 0 & 0 & P_I \end{pmatrix}, \quad A = \begin{pmatrix} A_I & 0 & 0 \\ 0 & A_I & 0 \\ 0 & 0 & A_I \end{pmatrix},$$

with

$$L_I = \begin{pmatrix} 0 & 1 & 1 \\ -1 & 0 & 0 \\ -1 & 0 & 0 \end{pmatrix}, \quad P_I = \begin{pmatrix} 0 & \sqrt{2} & \sqrt{2} \\ 1 & i & -i \\ -1 & i & -i \end{pmatrix},$$

$$P_I^{-1} = \begin{pmatrix} 0 & 1/2 & 1/2 \\ 1 & i & -i \\ -1 & i & -i \end{pmatrix}, \quad A = \begin{pmatrix} \nu & 0 & 0 \\ 0 & \nu c & 0 \\ 0 & 0 & \nu c \end{pmatrix},$$

the eigenvalues of L_I being, $0, \pm i\sqrt{2}$. The renormalized system which is linear reads, for $i = 1, 4, 7$:

$$\begin{aligned} \dot{U}_i + \frac{1}{2}\nu(1+c)U_i &= 0, \\ \dot{U}_{i+1} + \frac{1}{4}\nu(1+3c)U_{i+1} + \frac{1}{4}\nu(1-c)U_{i+2} &= 0, \\ \dot{U}_{i+2} + \frac{1}{4}\nu(1-c)U_{i+1} + \frac{1}{4}\nu(1+3c)U_{i+2} &= 0. \end{aligned} \quad (3.8)$$

Figure 4 shows the superposition of $u_1 = u_1^\varepsilon$ and $\bar{u}_1 = \bar{u}_1^\varepsilon$ and of $u_2 - u_3 = u_2^\varepsilon - u_3^\varepsilon$ with $\bar{u}_2 - \bar{u}_3 = \bar{u}_2^\varepsilon - \bar{u}_3^\varepsilon$; the computations were made for $\nu = 10^{-2}$, $F = 1$, $c = 1$, $\varepsilon = 5 \times 10^{-3}$

The analytical computations becoming somehow involved, they have been performed in this example with the help of the Maple program.

EXAMPLE 5. We conclude with an example for which L is symmetric semidefinite positive, while L was always antisymmetric in the previous examples.

The following example was introduced in [19] as a simplified model for the study of multilevel numerical methods adapted to the simulation of turbulence ; in the comparison with these algorithms (of the nonlinear Galerkin type), y represents the large scale component of the velocity and z represents its small scale component. Note the large ‘viscosity’ coefficient for z equal to $1/\varepsilon$, which produces the small-scale vortices (in agreement with the conventional theory of turbulence, see *e.g.* [20], [21]).

With $u = (y, z)$, this system reads

$$\begin{cases} \dot{y} + y + yz = f, \\ \dot{z} + \frac{1}{\varepsilon}z - y^2 = g. \end{cases} \quad (3.9)$$

Using the results of Section 2, we find the following renormalized system:

$$\begin{cases} \dot{Y} + Y = f, \\ \dot{Z} = 0. \end{cases} \quad (3.10)$$

Then, in the present case the approximate solution can be calculated analytically and it reads ($u_0 = (y_0, z_0)$):

$$\begin{aligned} \bar{y}^\varepsilon(t) &= f + (y_0 - f) e^{-t} + \varepsilon[f + (y_0 - f) e^{-t}]z_0(e^{-t/\varepsilon} - 1), \\ \bar{z}^\varepsilon(t) &= e^{-t/\varepsilon} [z_0 - \varepsilon[f + (y_0 - f) e^{-t}]^2 - \varepsilon g] + \varepsilon g + \varepsilon[f + (y_0 - f) e^{-t}]^2. \end{aligned} \quad (3.11)$$

Theorems 1 and 2 apply for all positive times. The expression above of $\bar{u}^\varepsilon = (\bar{y}^\varepsilon, \bar{z}^\varepsilon)$ shows the superposition of the large structures evolving on the time scale t and of small structures evolving on the time scales t and t/ε .

A straightforward computation gives the system of equations satisfied by $\bar{u}^\varepsilon = (\bar{y}^\varepsilon, \bar{z}^\varepsilon)$:

$$\begin{cases} \dot{\bar{y}}^\varepsilon + \bar{y}^\varepsilon + \bar{y}^\varepsilon \bar{z}^\varepsilon = f + \varepsilon R_1^\varepsilon(t), \\ \dot{\bar{z}}^\varepsilon + \frac{1}{\varepsilon} \bar{z}^\varepsilon - (\bar{y}^\varepsilon)^2 = g + \varepsilon R_2^\varepsilon(t), \end{cases} \quad (3.12)$$

where

$$\begin{aligned} R_1^\varepsilon(t) &= z_0(e^{-t/\varepsilon} - 1) (f + Y(t)z_0 e^{-t/\varepsilon}) \\ &\quad + Y(t)(Y(t)^2 + g)(1 - e^{-t/\varepsilon}) (1 + \varepsilon z_0(e^{-t/\varepsilon} - 1)), \end{aligned} \quad (3.13)$$

where $Y(t) = f + (y_0 - f)e^{-t}$, and

$$R_2^\varepsilon(t) = (1 - e^{-t/\varepsilon}) [2Y(t)(f - Y(t)) + 2Y(t)^2 z_0 + \varepsilon Y(t)^2 z_0^2 (1 - e^{-t/\varepsilon})]. \quad (3.14)$$

Note that \bar{y}^ε , \bar{z}^ε are bounded for all $t \geq 0$. Moreover, $R_1^\varepsilon(t)$ and $R_2^\varepsilon(t)$ are bounded for all $t \geq 0$, independently of ε , *i.e.*

$$\begin{cases} \sup_{t \geq 0} (|R_1^\varepsilon(t) + R_2^\varepsilon(t)|) \leq C(f, g, z_0, y_0), \\ \sup_{t \geq 0} (|\bar{y}^\varepsilon| + |\bar{z}^\varepsilon|) \leq C, \quad \sup_{t \geq 1/2} |\bar{z}^\varepsilon|(t) \leq C\varepsilon. \end{cases} \quad (3.15)$$

Estimates for $u^\varepsilon - \bar{u}^\varepsilon$

We set $p^\varepsilon = y^\varepsilon - \bar{y}^\varepsilon$ and $q^\varepsilon = z^\varepsilon - \bar{z}^\varepsilon$. Then $(p^\varepsilon, q^\varepsilon)$ satisfies:

$$\begin{cases} \dot{p}^\varepsilon + p^\varepsilon + p^\varepsilon q^\varepsilon + \bar{z}^\varepsilon p^\varepsilon + \bar{y}^\varepsilon q^\varepsilon = -\varepsilon R_1^\varepsilon, \\ \dot{q}^\varepsilon + \frac{1}{\varepsilon} q^\varepsilon - (p^\varepsilon)^2 + 2\bar{y}^\varepsilon p^\varepsilon = -\varepsilon R_2^\varepsilon, \end{cases} \quad (3.16)$$

with the initial conditions $p^\varepsilon(0) = 0$, $q^\varepsilon(0) = 0$. Multiplying the first equation by p^ε and the second equation by q^ε , we obtain after adding:

$$\frac{1}{2} \frac{d}{dt} [(p^\varepsilon)^2 + (q^\varepsilon)^2] + (p^\varepsilon)^2 + \frac{1}{\varepsilon} (q^\varepsilon)^2 + \bar{z}^\varepsilon (p^\varepsilon)^2 + 3\bar{y}^\varepsilon p^\varepsilon q^\varepsilon = -\varepsilon [p^\varepsilon R_1^\varepsilon + q^\varepsilon R_2^\varepsilon],$$

which leads to

$$\begin{aligned} &\frac{1}{2} \frac{d}{dt} [(p^\varepsilon)^2 + (q^\varepsilon)^2] + (p^\varepsilon)^2 + \frac{1}{\varepsilon} (q^\varepsilon)^2 \\ &\leq \frac{1}{2} \left[(p^\varepsilon)^2 + \frac{1}{\varepsilon} (q^\varepsilon)^2 \right] + |\bar{z}^\varepsilon| (p^\varepsilon)^2 + \kappa \varepsilon (\bar{y}^\varepsilon)^2 (p^\varepsilon)^2 + \kappa \varepsilon^2 (R_1^\varepsilon)^2 + \kappa \varepsilon^3 (R_2^\varepsilon)^2. \end{aligned}$$

Therefore, taking into account (3.15), we deduce that

$$\frac{d}{dt} [(p^\varepsilon)^2 + (q^\varepsilon)^2] + (p^\varepsilon)^2 + \frac{1}{\varepsilon} (q^\varepsilon)^2 \leq \kappa (p^\varepsilon)^2 + \kappa \varepsilon^2 \quad \text{for } t \geq 0,$$

and

$$\frac{d}{dt} [(p^\varepsilon)^2 + (q^\varepsilon)^2] + (p^\varepsilon)^2 + \frac{1}{\varepsilon} (q^\varepsilon)^2 \leq \kappa \varepsilon (p^\varepsilon)^2 + \kappa \varepsilon^2 \quad \text{for } t \geq \frac{1}{2},$$

where κ is a constant depending on the data, but not on ε . Hence, there exists an $\varepsilon_0 = \varepsilon_0(f, g, y_0, z_0) = \frac{1}{2\kappa}$ such that if $\varepsilon \leq \varepsilon_0$, then

$$\begin{cases} \frac{d}{dt} [(p^\varepsilon)^2 + (q^\varepsilon)^2] \leq \kappa (p^\varepsilon)^2 + \kappa \varepsilon^2 \quad \text{for } t \geq 0 \\ \frac{d}{dt} [(p^\varepsilon)^2 + (q^\varepsilon)^2] + \frac{1}{2} [(p^\varepsilon)^2 + \frac{1}{\varepsilon} (q^\varepsilon)^2] \leq \kappa \varepsilon^2, \quad \text{for } t \geq \frac{1}{2}. \end{cases} \quad (3.17)$$

Let T^ε be the first time such that $|p^\varepsilon|^2 + |q^\varepsilon|^2 = \kappa\varepsilon^2$; we have for $t \leq T^\varepsilon$:

$$|p^\varepsilon(t)|^2 + |q^\varepsilon(t)|^2 \leq \kappa\varepsilon^2 t.$$

Hence $T^\varepsilon > \frac{1}{2}$ and we have

$$|p^\varepsilon(t)|^2 + |q^\varepsilon(t)|^2 \leq 2\kappa\varepsilon^2, \quad \text{for } 0 \leq t \leq \frac{1}{2}.$$

Now starting at $t = \frac{1}{2}$, we use the Gronwall lemma and obtain

$$|p^\varepsilon(t)|^2 + |q^\varepsilon(t)|^2 \leq |p^\varepsilon(\frac{1}{2})|^2 + |q^\varepsilon(\frac{1}{2})|^2 + \kappa\varepsilon^2 \leq 3\kappa\varepsilon^2, \quad \text{for } t \geq \frac{1}{2}.$$

Hence

$$(p^\varepsilon)^2 + (q^\varepsilon)^2 \leq 3\kappa\varepsilon^2, \quad \forall t \geq 0. \tag{3.18}$$

We also deduce from (3.16)₂ and (3.18) that

$$\frac{d}{dt}(q^\varepsilon)^2 + \frac{1}{\varepsilon}(q^\varepsilon)^2 \leq \kappa\varepsilon(p^\varepsilon)^2 + \kappa\varepsilon(p^\varepsilon)^4 + \kappa\varepsilon^3 \leq \kappa\varepsilon^3,$$

so that, by applying again the Gronwall lemma, we find the following estimate for q^ε :

$$(q^\varepsilon)^2 \leq \kappa\varepsilon^4, \quad \forall t \geq 0. \tag{3.19}$$

We conclude that

$$\begin{cases} \sup_{t \geq 0} |y^\varepsilon - \bar{y}^\varepsilon| \leq \kappa\varepsilon, \\ \sup_{t \geq 0} |z^\varepsilon - \bar{z}^\varepsilon| \leq \kappa\varepsilon^2. \end{cases} \tag{3.20}$$

4. Concluding remarks

In this article we have presented some preliminary results concerning an averaging (smoothing) procedure which is being developed by us. We have not been able to include here the details of the analysis and the proof of the results which are lengthy and hinge on functional-analysis tools; this will appear in subsequent articles, as well as the application to larger systems corresponding, for instance, to the spatial discretization of partial differential equations.

In all the examples we have been able to replace the integration of a very oscillatory system requiring a small time step by that of a nonoscillatory one allowing a much larger time step and we were nevertheless able to recover almost all the details of the oscillations. Of course, the systems considered are extremely simple, but we are optimistic and believe that the method will still be effective for much larger systems. There is also the intriguing question of the approximation, sometimes, of an oscillatory nonlinear system by a linear one which needs to be investigated.

Acknowledgments

This work was partly supported by the National Science Foundation under the Grant NSF-DMS-9400615 and by the Research Fund of Indiana University.

References

1. H. Poincaré, *Les Méthodes Nouvelles de la Mécanique Céleste*. T.1, New-York: Dover (1957) 382 pp.
2. E. N. Lorenz, On the existence of a slow manifold. *J. Atmos. Sci.* 43 (1986) 1547–1557.
3. L. I. Chen, N. Goldenfeld and Y. Oono, The renormalization group and singular perturbations: multiple-scales, boundary layers and reductive perturbation theory. *Physical Reviews E* 54 (1997) 376–394.
4. M. Ziane, The connection between the renormalization group method and the Poincaré Dulac theory. Preprint, Institute for Scientific Computing and Applied Mathematics, Indiana University (1997) 17 pp.
5. V. Yakhot, and S.A. Orszag, Renormalization group analysis of turbulence. I. Basic Theory. *J. Sci. Comp.* 1 (1986) 3–51.
6. J. D. Cole, and J. Kevorkian, *Perturbation Methods in Applied Mathematics*. Berlin: Springer-Verlag (1981) 558 pp.
7. A. Babin, A. Mahalov, and B. Nicolaenko, Global splitting, integrability and regularity of 3D Euler and Navier-Stokes equations for uniformly rotating fluids. *Eur. J. Mech.B/Fluids* 15 (1996) 291–300.
8. A. Babin, A. Mahalov and B. Nicolaenko, Integrability and regularity of 3D Euler and equations for uniformly rotating fluids. *Comp. Math. Appl.* 31 (1996) 35–42.
9. I. Gallagher, Existence globale pour des équations des fluides géostrophiques. *C.R. Acad. Sci. Paris*, t.325, Série I (1997) 623–626.
10. J. Bricmont, and A. Kupiainen, Renormalizing partial differential equations, *Constructive Physics*, Palaiseau, 1994. In: *Lectures Notes in Physics*, n° 446. New-York: Springer-Verlag (1995) pp. 83–115.
11. J. L. Bona, K. S. Promislow, and C. E. Wayne, Higher order asymptotics of decaying solutions of some nonlinear, dispersive, dissipative equations. *Nonlinearity* 8 (1995) 1179–1206.
12. J. L. Bona, K. S. Promislow, and C. E. Wayne, On the asymptotic behavior of solutions to nonlinear, dispersive, dissipative wave equations. *Math. Comput. Simul.* 37 (1994) 265–277.
13. L. R. Petzold, L. O. Jay, and J. Yen, Numerical solutions of highly oscillatory ordinary differential equations. *Acta Numerica* (1997) 437–483.
14. J. Pedlovsky, *Geophysical Fluid Dynamics*. New York: Springer-Verlag (1987) 710 pp.
15. V. I. Arnold, *Geometric Methods in the Theory of Ordinary Differential Equations*. New-York: Springer-Verlag (1988) 351 pp.
16. V. I. Arnold, *Mathematical Methods of Classical Mechanics*. New-York: Springer-Verlag (1989) 508 pp.
17. A. Bensoussan, J. L. Lions, and G. Papanicolaou, *Asymptotic Analysis for Periodic Structures*, 5. Amsterdam: North Holland (1978) 700 pp.
18. I. Moise and M. Ziane, renormization group method. Application to PDE to appear.
19. R. Temam, Multilevel methods for the simulation of turbulence, A simple model. *J. Comp. Phys.* 127 (1996) 309–315.
20. G. K. Batchelor, *The Theory of Homogeneous Turbulence*. Cambridge: Cambridge University Press (1967) 615 pp.
21. S. A. Orszag, Lectures on the statistical theory of turbulence Proceedings, In: *Summer School of Theoretical Physics, Les Houches*. London: Gordon and Breach (1973) pp. 235–374.